An articulated assistive robot for intuitive hands-on-payload manipulation

Article *in* Robotics and Computer-Integrated Manufacturing · April 2017

DOI: 10.1016/j.rcim.2017.04.003

7 authors, including:

Alexandre Campeau-Lecours
Laval University
44 PUBLICATIONS **181** CITATIONS
SEE PROFILE

Dalong Gao
General Motors Company
23 PUBLICATIONS **158** CITATIONS
SEE PROFILE

Clément Gosselin
Laval University
573 PUBLICATIONS **17,557** CITATIONS
SEE PROFILE

An articulated assistive robot for intuitive hands-on-payload manipulation

This paper is a Post-Print version (ie final draft post-refereeing). For access to Publishers version, please access http://doi.org/10.1016/j.rcim.2017.04.003.

Alexandre Campeau-Lecours[a,*], Pierre-Luc Belzile[a], Thierry Laliberté[a], Simon Foucault[a], Boris Mayer-St-Onge[a], Dalong Gao[b], Clément Gosselin[a]

[a] *Département de génie mécanique, Université Laval, Québec, Canada*
[b] *GM Global Research, Warren, Michigan, USA*

Abstract

This paper presents an intelligent assistive robot designed to help operators in lifting and moving large payloads through direct physical contact (hands-on-payload mode). The mechanical design of the robot is first presented. Although its kinematics are similar to that of a cable-suspended sytem, the proposed mechanism is based on articulated linkages, thereby allowing the payload to be offset from the rail support on which it is suspended. A dynamic model of the robot is then developed. It is shown that a simplified dynamic model can be obtained using geometric assumptions. Based on the simplified dynamic model, a controller is then presented that handles the physical human-robot interaction and that provides the operator with an intuitive direct control of the payload. Experimental validation on a full-scale prototype is presented in order to demonstrate the effectiveness of the proposed robot and controller.

Keywords: Physical Human-Robot Interaction, Assistive robots, Intelligent assist device, Robotic assembly, Robotics

1. INTRODUCTION

Assistive devices are used in many industrial applications to help operators moving and lifting payloads. The objective is to combine the force capabilities of such devices with the decision and adaptation capabilities of a human

*Corresponding author
Email addresses: alexandre.campeau-lecours@gmc.ulaval.ca (Alexandre Campeau-Lecours), pierre-luc.belzile.1@ulaval.ca (Pierre-Luc Belzile), Thierry.Laliberte@gmc.ulaval.ca (Thierry Laliberté), foucault@gmc.ulaval.ca (Simon Foucault), Boris.Mayer-St-Onge@gmc.ulaval.ca (Boris Mayer-St-Onge), dalong.gao@gm.com (Dalong Gao), clement.gosselin@gmc.ulaval.ca (Clément Gosselin)

operator. This approach allows to perform tasks that are too complex for automated systems but that raise ergonomic issues, preventing them from being performed manually. Such systems are often referred to as Intelligent Assist Devices (IAD) or Assistive Robots (AR) and are used in many industrial [1, 2] and rehabilitation [3] applications.

Assistive robots relate to the broader field of physical human-robot interaction (pHRI) and may be classified in two main classes, namely: hands-on-handle systems and hands-on-payload systems [2]. Hands-on-handle systems require the operator to interact through a specific point on the device. Typically, a handle equipped with a force sensor allows the operator to move the robot and the payload. Examples of such robotic devices are described in [4, 2]. On the other hand, hands-on-payload systems allow the operator to physically interact directly with the payload. By being in close contact with the payload, its manipulation becomes much more intuitive. The operator can also change the position of his hands on the payload in order to be more efficient, productive, comfortable or to have a clearer view of the task at hand. Similarly, the operator can also use only one hand while the other is used for another aspect of the task [5, 2]. Finally, this arrangement allows several operators to interact with a same payload.

Typical hands-on-payload systems are based on cable-suspended assist devices such as in [6, 2, 7, 8, 9, 10]. When the operator pushes the payload, the cable deviates from the vertical direction and this deviation is measured by a cable angle sensor. The controller's objective, by using the cable angle as an input, is to assist the operator in moving the payload in the horizontal plane while controlling cable sway. Vertical assistance is normally achieved by placing a force sensor in-line with the cable and by implementing force control algorithms [6, 11, 12, 13, 14]. In addition to providing a hands-on-payload mode, cable-suspended systems present many advantages such as a free rotation, reduced inertia, reduced cost and a compact structure [6, 2]. However, the payload's centre of mass must be aligned with the cable which is an issue in many applications. First, some applications require to place the payload inside an object such as the body of a car, which is not possible since the cable would interfere with the said object. Other applications require to insert the payload with a specific orientation, which is not possible because of the alignment of the centre of mass of the payload with the cable. For these applications, a hands-on-handle system is thus normally used.

The objective of this work is to combine the advantages of hands-on-handle and hands-on-payload cable-suspended systems by providing a hands-on-payload solution while allowing payload centre of mass offset. The motivation is to extend the range of applications in which hands-on-payload systems can be implemented, including assembly and part insertion. The principle of the proposed assistive robot is similar to that of cable-suspended systems [6] but an articulated mechanism is used instead of a cable, as shown in Fig. 1. This type of mechanism have been applied to assembly applications [15, 16]. By pushing the payload, the operator imparts a motion to the mechanism, which is measured using joint encoders. The control system's objective, by moving an overhead

Figure 1: Prototype of an articulated intelligent assistive robot.

cart, is mainly to keep the mechanism links vertical. The cart thus moves in the direction desired by the operator while damping the link oscillations, resulting in a safe assistance to the operator. The payload can be offset from the mechanism centre thanks to the mechanism structure.

The paper is structured as follows. The design of the articulated mechanism is first presented. Then, the system's complete dynamic model and its controller are described. Finally, experiments performed on an industrial-scale prototype are conducted to show the system's performance.

2. Design of the assistive robot

2.1. Articulated passive mechanism

At the core of the proposed robot is the concept of a two-degree-of-freedom suspended articulated passive mechanism. The proposed mechanism consists of two four-bar linkages mounted in series and moving in orthogonal vertical planes, as illustrated schematically in Fig. 2. In order to withstand large external forces and torques, each four-bar linkage is doubled and attached with additional links, as shown in Fig. 3. The articulated mechanism possesses the same degrees of freedom (dof) as cable-suspended systems. However, due to the rigid links, the payload can be offset from the mechanism centre (Fig. 3) or from the payload's attachment point (Fig. 4). This is an important advantage over cable-suspended intelligent assistive devices [6] in which the centre of mass of the payload must necessarily be aligned with the cable, thus limiting the potential applications.

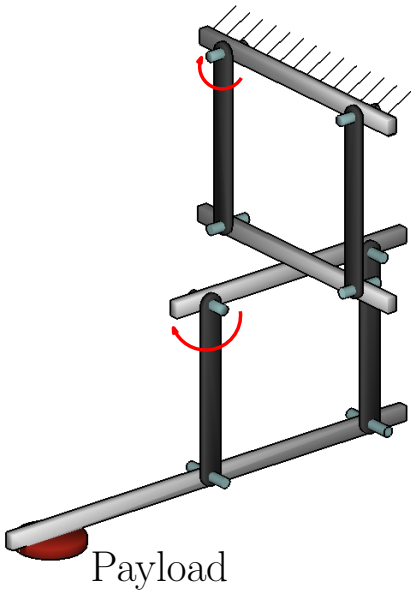

Figure 2: Basic principle of the double four-bar articulated passive suspended mechanism.

The natural frequency of the suspended passive mechanism is determined by the vertical link lengths, which is thus an important design parameter. Longer links reduce the natural frequency, which is then easier for the controller to cope with. However, longer links are more cumbersome. Experiments with different link lengths have shown that link lengths of $0.4m$ represent a good compromise for our specific prototype. It is pointed out that,similarly to a simple pendulum, the payload mass does not affect the four bar natural oscillation frequency. Additionally, thanks to the four-bar configuration, the vertical payload offset (L_5) does not affect the natural four-bar mechanism oscillation frequency either (see eqns. (7) and (8) of the dynamical model in section III.A). The mechanism structure is attached to a bridge crane, as shown in Fig. 1, allowing horizontal (X and Y) motions along with a vertical (Z) motion and a rotation (ϕ_c) around the vertical axis.

The proposed mechanism allows to infer the human intentions by detecting the link deviations from the vertical direction. In the absence of external forces, gravity maintains the links in their neutral position. In order to reduce the force required to impart a movement to the links, it is then important to reduce the static friction as much as possible. To this end, roller bearings are used at each joint. It would also be possible to add viscous dampers to the joints in order to help the controller by mechanically damping the oscillations.

Instead of such an articulated mechanism, a mechanism consisting of horizontal linear guides could have been used. In this concept, springs would be used to maintain the system in a neutral position and human intentions would be detected by measuring the deviation from this neutral position. Although

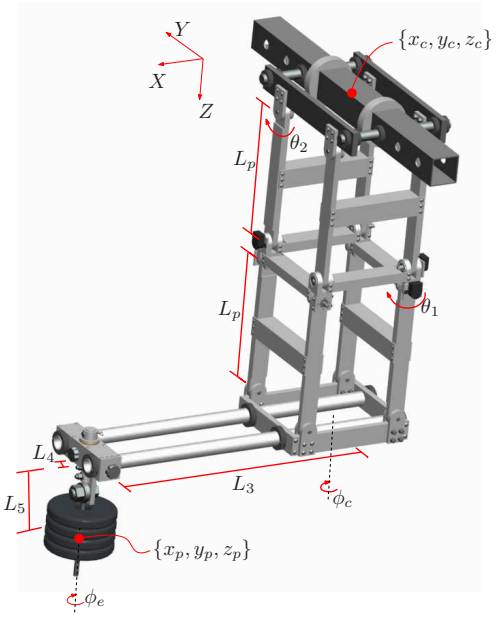

Figure 3: CAD model of the articulated suspended passive mechanism and definition of the geometric parameters.

this solution may seem simpler than the articulated mechanism solution, the latter presents important practical advantages. Indeed, the linear system may be more prone to static friction and the natural frequency of the passive linear mechanims would depend on the payload mass. The controller would then need to be adapted online for different payload mass.

Figure 4: Offset of the attachment point of the payload.

2.2. Model parameters

The geometric parameters of the mechanism are shown in Figs. 3 and 6. L_p refers to the vertical link length, L_3, L_4 and L_5 are the distances between the mechanism centre (point C) and the payload centre of mass respectively in the

X' and Y' direction. The global frame is represented by the $[X, Y, Z]$ frame and the moving frame by the $[X', Y', Z']$ frame where X' is aligned with the tubes (see Fig. 6(c)). The centre position of the actuated cart supporting the passive mechanism and the position of the payload are expressed in the moving frame and are noted x_c, y_c, z_c and x_p, y_p, z_p respectively. Angles θ_1 and θ_2 are the passive mechanism's joint angles, ϕ_c is the mechanism rotation about the vertical axis and ϕ_e is the payload vertical rotation about the end-effector axis (shown in Fig. 3).

2.3. Sensors

Because there are several revolute joints in the passive mechanism, several sensors can be used, such as relative encoders, Hall effect sensors, absolute encoders, potentiometers, accelerometers, gyroscopes and photointeruptors. In this paper, an encoder and a Hall effect sensor are used for each of the two degrees of freedom of the passive mechanism. The signals are fused using a Kalman filter with a third order acceleration model [17] are compared to detect possible faults. Fig. 5 shows an example of the fusion.

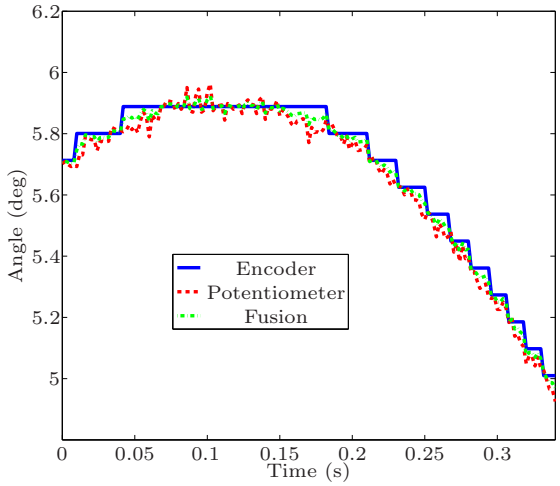

Figure 5: Sensor fusion exemple between an incremental encoder and a Hall effect sensor.

3. DYNAMICS AND CONTROL

In the following, the equations of motion are developed. The equations are first obtained with a complete model referred to as *coupled motion* and then, with simplifications, a *simplified model* is obtained.

3.1. COUPLED MOTION

3.1.1. EQUATIONS OF MOTION

In this work, the payload vertical position is fixed. However, it would be possible to integrate vertical motions to this design. There are two main options: (1) the vertical actuation could be performed at the end effector (for instance at mass m position in Fig.6 (2) above the articulated mechanism. The equations of motion would differ between both cases. In this paper, for the sake of completeness in developing the dynamical equations, the equations were developed by considering a vertical actuation controlling the payload position Z_c at the end effector.

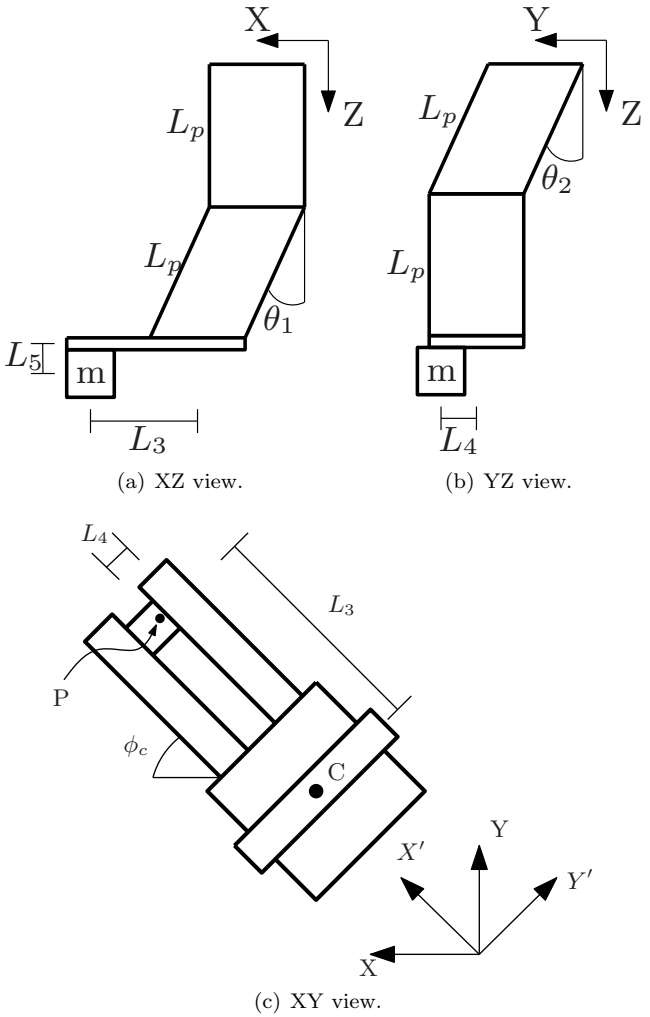

(a) XZ view.

(b) YZ view.

(c) XY view.

Figure 6: Geometric parameters of the articulated mechanism.

With the parameters defined in Figs. 3 and 6, the following velocities are obtained

$$\begin{aligned}
\dot{x}_p &= \dot{x}_c + L_p\dot{\theta}_1\cos\theta_1 - L_4\dot{\phi}_c \\
\dot{y}_p &= \dot{y}_c + L_p\dot{\theta}_2\cos\theta_2 + L_3\dot{\phi}_c \\
\dot{z}_p &= \dot{z}_c - L_p\dot{\theta}_1\sin\theta_1 - L_p\dot{\theta}_2\sin\theta_2 \\
\dot{\phi}_p &= \dot{\phi}_c + \dot{\phi}_e.
\end{aligned} \tag{1}$$

The potential energy is written as

$$V = -mgL_p(\cos\theta_1 + \cos\theta_2) - z_c \tag{2}$$

where m is the payload mass and the kinetic energy is written as

$$\begin{aligned}
T = \frac{1}{2}M_x\dot{x}_c^2 + \frac{1}{2}M_y\dot{y}_c^2 + \frac{1}{2}M_z\dot{z}_c^2 + \\
\frac{1}{2}m(\dot{x}_p^2 + \dot{y}_p^2 + \dot{z}_p^2) + \frac{1}{2}i_e\dot{\phi}_p^2.
\end{aligned} \tag{3}$$

where M_x, M_y and M_z are the cart's effective mass respectively in the X', Y' and Z' direction[1]. The mass of the articulated links is neglected here. From eqns. (2) and (3) and using the Lagrange method, the equations of motion are:

$$\begin{aligned}
F_X &= M_x\ddot{x}_c + m(\ddot{x}_c - L_p\dot{\theta}_1^2\sin\theta_1 \\
&\quad + L_p\ddot{\theta}_1\cos\theta_1 - L_4\ddot{\phi}_c)
\end{aligned} \tag{4}$$

$$\begin{aligned}
F_Y &= M_y\ddot{y}_c + m(\ddot{y}_c - L_p\dot{\theta}_2^2\sin\theta_2 \\
&\quad + L_p\ddot{\theta}_2\cos\theta_2 + L_3\ddot{\phi}_c)
\end{aligned} \tag{5}$$

$$\begin{aligned}
F_Z &= M_z\ddot{z}_c + m(\ddot{z}_c - L_p\dot{\theta}_1^2\cos\theta_1 \\
&\quad - L_p\ddot{\theta}_1\sin\theta_1 - L_p\dot{\theta}_2^2\cos\theta_2 - L_p\ddot{\theta}_2\sin\theta_2 - g)
\end{aligned} \tag{6}$$

$$\begin{aligned}
0 &= mL_p(\ddot{x}_c\cos\theta_1 - L_4\ddot{\phi}_c\cos\theta_1 - \ddot{z}_c\sin\theta_1 \\
&\quad + L_p\ddot{\theta}_1 + L_p\dot{\theta}_2^2\sin\theta_1\cos\theta_2 + L_p\ddot{\theta}_2\sin\theta_1\sin\theta_2 \\
&\quad + g\sin\theta_1)
\end{aligned} \tag{7}$$

$$\begin{aligned}
0 &= mL_p(\ddot{y}_c\cos\theta_2 + L_3\ddot{\phi}_c\cos\theta_2 - \ddot{z}_c\sin\theta_2 \\
&\quad + L_p\ddot{\theta}_2 + L_p\dot{\theta}_1^2\sin\theta_2\cos\theta_1 + L_p\ddot{\theta}_1\sin\theta_1\sin\theta_2 \\
&\quad + g\sin\theta_2).
\end{aligned} \tag{8}$$

where F_X is the X' axis trolley force, F_Y is the Y' axis trolley force, F_Z is the vertical force and the last two equations represent the dynamics of the passive double pendulum. Globally, the system has five degrees of freedom (the rotation

[1]The effective mass of the cart can be different in each direction since a bridge and trolley system is typically used to move in the horizontal plane.

around the vertical axis is not considered) and three controlled inputs, namely the X, Y and Z motions of the trolley.

From eqns. (4) to (8) and namely from eqn. (8), it can be observed that the coupling between the joint angles is negligible for relatively small angles, angular velocities and for low angular acceleration $\ddot{\phi}_c$. Thus, neglecting the coupling effects, a simplified model can be obtained in which the X and Y motions are treated separately, as shown in the next section.

3.2. SIMPLIFIED MODEL

Considering only one degree of freedom (e.g. the X axis as shown in Fig. 7), the equations of motion are reduced to:

$$F_X = (M_x + m)\ddot{x} + m\ddot{\theta}_1 L_p \cos\theta_1 - mL_p\dot{\theta}_1^2 \sin\theta_1 \quad (9)$$

$$0 = (\ddot{x}\cos\theta_1 + g\sin\theta_1 + L_p\ddot{\theta}_1)mL_p \quad (10)$$

where M_x is the cart mass is the X direction, m is the payload mass and where L_p is constant. Assuming small angles and neglecting $\dot{\theta}_1^2$, the equations can be linearized as:

$$F_x = (M_x + m)\ddot{x} + m\ddot{\theta}_1 L_p \quad (11)$$

$$0 = \ddot{x} + g\theta_1 + L_p\ddot{\theta}_1 \quad (12)$$

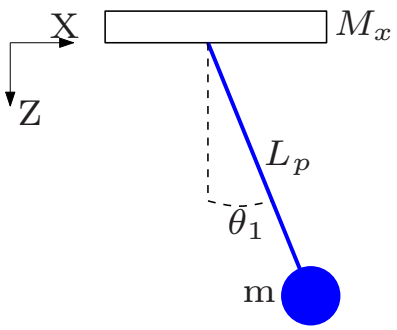

Figure 7: Definition of the parameters for the simplified model.

3.3. CONTROL

Two horizontal control modes are implemented: cooperation and autonomous mode. In both cases, the system measures the link angles and the controller's objective is to keep the links vertical by moving the overhead cart. In cooperation mode, the operator imparts an angle to the links by pushing on the payload. The controller thus moves the overhead cart in the direction desired by the operator, while controlling the link sway, resulting in an intuitive assistance to the operator. Additionally, since the controller's objective is to maintain the links vertical, the operator does not need to stop the load himself, which could

otherwise raise ergonomic issues. Finally, in the autonomous mode, the cart is moving by itself to reach a prescribed position while controlling the link sway. The controller uses a scheme previously developed for a cable-based system and specifically designed for human assistance [6, 18]. This controller is based on a state-space controller using the *simplified model*. The proposed methodology is to use a backstepping approach [19, 20] to decouple the control problem into two controllers which provides many advantages [6, 14]. The general control scheme is shown in Fig. 8.

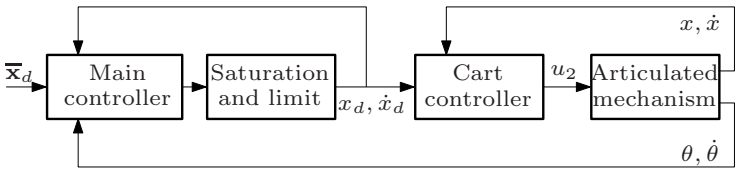

Figure 8: General control scheme.

3.3.1. MODE SWITCHING

When switching from a given mode (cooperation or autonomous) to another, large accelerations and jerks may be obtained and bumpless control transfer must then be considered. Different classical approaches are possible such as storing the last control input or using an observer. However, classical methods are more difficult to properly implement in practice because of the need to switch between the autonomous mode (which is position controlled) and a human cooperation mode (which is velocity controlled).

The proposed method first consists in storing the measured velocity when a mode switch is required. When switching to cooperation mode, which uses velocity control, we use:

$$v_{out} = a_m v_0 + (1 - a_m) v_d \tag{13}$$

where v_{out} is the desired velocity output of the mode switching algorithm, v_d is the current desired velocity and v_0 is the measured velocity at the mode switch time. The variable a_m is reinitialized at 1 when a mode switch is taking place and is then multiplied by b_m (a design parameter) at each time step, namely:

$$a_m(k) = a_m(k-1) b_m. \tag{14}$$

At first, v_{out} is equal to the initial measured velocity (v_0) and after some time a_m decays to 0 and thus v_{out} decays to v_d. The idea is to smoothly transition from the measured velocity at the mode switch moment (v_0) to the desired velocity (v_d) of the controller. Figure 9 shows an example of a transition witout and with bumpless transfer. In the first case, without bumpless transfer, the transition is agressive. In the second case, the transition is more smooth and the robot returns to a zero velocity faster and more smoothly.

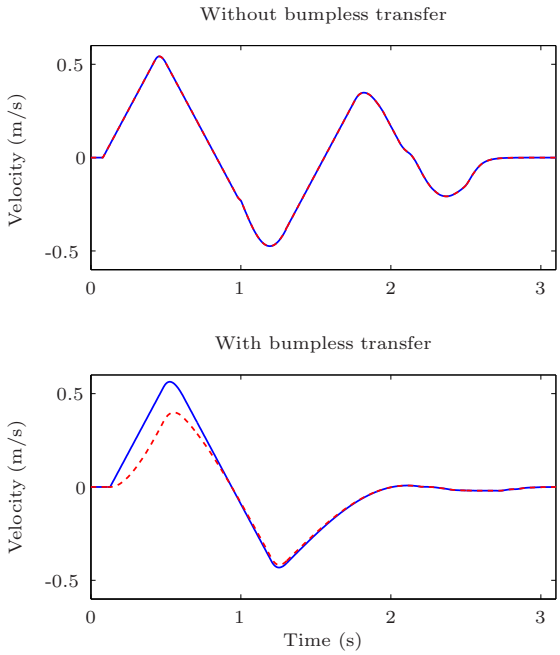

Figure 9: Bumpless transfer example with $b_m = 0.995$ with $T_s = 2ms$. The blue line is the desired velocity while the red dashed line is the mode switch output velocity.

4. EXPERIMENTATION

Experiments were performed using the industrial-scale gantry system shown in Fig. 1 [4]. The total moving mass is approximately $350kg$ in the direction of the X axis and $170kg$ along the Y axis. The payload may vary between 0 and $50kg$ (a $23kg$ payload is used in the experiments) and the horizontal workspace is $3.3m \times 2.15m$. The controller is implemented on a real-time QNX computer with a sampling period of 2ms. The algorithms are programmed using Simulink/RT-LAB software. The accompanying video shows excerpts of the experiments.

4.1. COOPERATION MODE

Two experiments were conducted using the cooperation mode: motion assistance and a recovery from an impulse in the X direction. The algorithm performance and stability was also experimentally verified in both directions separately and with motions occurring in both directions simultaneously.

The first experiment consisted in performing usual motions in order to assess the system assistance to the operator and the results are shown in Fig. 10. The required force with a $23kg$ payload located at $X_p = 0.74m$ (shown in Tab. 1) for precise motions ($0.2m/s$) is $10N$ while the required force for faster motions ($0.6m/s$) is $32N$. The force was measured with a 6 axis ATI force sensor to assess

the system performances but the force sensor was not used by the controller. Additionally, the system automatically brings the links to the vertical position and thus the operator does not have to stop the payload, which could otherwise raise ergonomic issues [2].

The second experiment, a recovery from an impulse, consisted in giving a large impulse to the payload in order to test the controller's ability to bring the mechanism links back to the vertical position. The results are shown in Fig. 11 where the links return to vertical position rapidly and smoothly. As explained in the preceding sections, it is pointed out that that mechanism design makes the link oscillations independant of the payload mass and payload offset. The same control gains, for the main controller, can thus be used for different payload mass and offset.

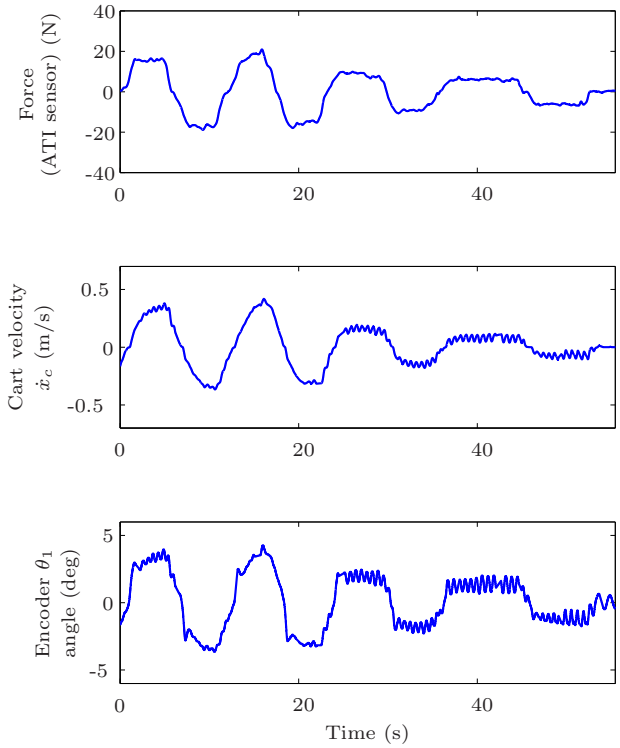

Figure 10: Interaction experiment. The figure shows the relation between the force applied by the human operator, the resulting cart velocity and the mechanism link's angle.

4.2. AUTONOMOUS MODE

The autonomous mode experiment consisted in prescribing a position while damping link oscillations. The first experiment only considered the prescribed position without considering the link angles. The second experiment was conducted with the controller described in section 3.3 with a damping ζ_1 of 0.9

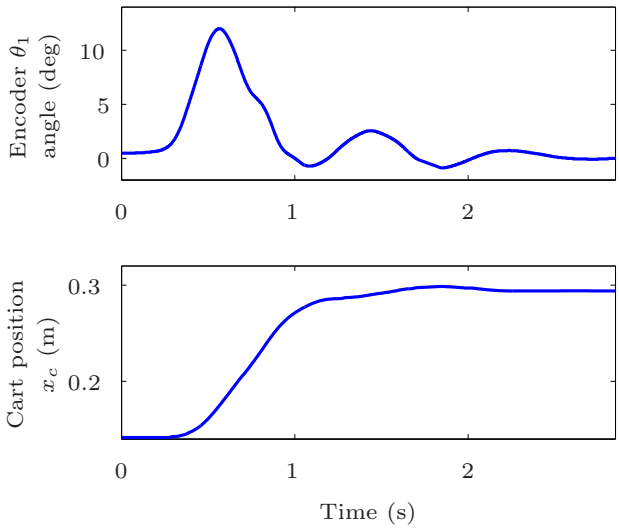

Figure 11: Horizontal impulse experiment.

Table 1: Required force for horizontal motion

Parameter	Unit	Value
Payload at 0.74m	kg	23
Precise motion (0.2 m/s)	N	10
Faster motion (0.6 m/s)	N	32

(see [6] for details). The results are shown in Fig. 12. In the first case, the link oscillations were obviously large while the cart position motion was very smooth. In the second case, the links oscillations were kept to minimal values while, as a compromise, the cart motion was more jerky. The accompanying video shows a visual result of the experiment.

CONCLUSION

This paper proposed an assistive robot based on a suspended passive articulated mechanism. The articulated mechanism was first presented along with the dynamic model and the controller. Experiments performed on an industrial-scale prototype were also conducted to demonstrate the system's performance. The proposed system combines the advantages of cable-suspended systems while allowing an offset of the payload centre of mass. The assistive robot thus allows to extend hands-on-payload systems to applications, such as assembly and part insertion, that were not possible before.

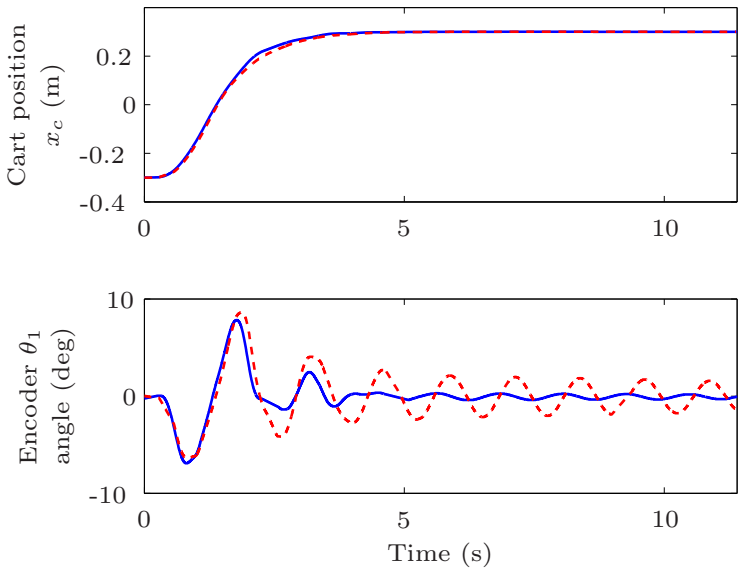

Figure 12: Autonomous mode experiment. The solid blue line uses the controller describe in this paper while the red dashed-line uses a simple position controller without considering the link angles.

This work focused on horizontal assistance while future work will focus on integrating vertical assistance.

Acknowledgment

This work was supported by The Natural Sciences and Engineering Research Council of Canada (NSERC) as well as by the Canada Research Chair Program and General Motors (GM) of Canada.

References

[1] J. Kruger, T. Lien, A. Verl, Cooperation of human and machines in assembly lines, {CIRP} Annals - Manufacturing Technology 58 (2) (2009) 628 – 646.

[2] A. Bicchi, M. A. Peshkin, J. E. Colgate, Safety for physical human-robot interaction, in: B. Siciliano, O. Khatib (Eds.), Springer Handbook of Robotics, Springer Berlin Heidelberg, 2008, pp. 1335–1348.

[3] A. Campeau-Lecours, V. Maheu, S. Lepage, H. Lamontagne, S. Latour, L. Paquet, N. Hardie, Jaco assistive robotic device: Empowering people with disabilities through innovative algorithms, in: Rehabilitation Engineering and Assistive Technology Society of North America (RESNA) annual conference, 2016.

[4] C. Gosselin, T. Laliberte, B. Mayer-St-Onge, S. Foucault, A. Lecours, V. Duchaine, N. Paradis, D. Gao, R. Menassa, A friendly beast of burden: A human-assistive robot for handling large payloads, IEEE Robotics Automation Magazine 20 (4) (2013) 139–147.

[5] J. E. Colgate, M. Peshkin, S. H. Klostermeyer, Intelligent assist devices in industrial applications: A review, in: IEEE/RSJ International Conference on Intelligent Robots and Systems, Las Vegas, Nevada, 2003.

[6] A. Campeau-Lecours, S. Foucault, T. Laliberté, B. Mayer-St-Onge, C. Gosselin, A cable-suspended intelligent crane assist device for the intuitive manipulation of large payloads, IEEE/ASME Transactions on Mechatronics 21 (4) (2016) 2073–2084.

[7] A. Lecours, S. Foucault, T. Laliberte, C. Gosselin, B. Mayer-St-Onge, D. Gao, R. J. Menassa, Movement system configured for moving a payload in a plurality of directions, US Patent 8,985,354 (Mar. 24 2015).

[8] H. Kazerooni, Exoskeletons for human performance augmentation, in: B. Siciliano, O. Khatib (Eds.), Springer Handbook of Robotics, Springer Berlin Heidelberg, 2008, pp. 773–793.

[9] E. Colgate, P. Decker, S. Klostermeyer, A. Makhlin, D. Meer, J. Santosmunne, M. Peshkin, M. Robie, Methods and apparatus for manipulation of heavy payloads with intelligent assist devices, US Patent 7,185,774 (2008).

[10] J. Wen, D. Popa, G. Montemayor, P. Liu, Human assisted impedance control of overhead cranes, in: Proceedings of the IEEE International Conference on Control Applications, 2001, pp. 383 –387.

[11] A. Lecours, B. Mayer-St-Onge, C. Gosselin, Variable admittance control of a four-degree-of-freedom intelligent assist device, in: IEEE International Conference on Robotics and Automation (ICRA), 2012.

[12] W. Wannasuphoprasit, J. Colgate, D. Meer, M. Peshkin, Method and apparatus for a high-performance hoist, US Patent 6,241,462 (2001).

[13] F. Dimeas, P. Koustoumpardis, N. Aspragathos, Admittance neuro-control of a lifting device to reduce human effort, Advanced Robotics 27 (13) (2013) 1013–1022.

[14] A. Lecours, C. Gosselin, Computed-torque control of a four-degree-of-freedom admittance controlled intelligent assist device, in: Experimental Robotics, Vol. 88 of Springer Tracts in Advanced Robotics, Springer International Publishing, 2013, pp. 635–649.

[15] P. D. Labrecque, J. M. Hache, M. Abdallah, C. Gosselin, Low-impedance physical human-robot interaction using an active passive dynamics decoupling, IEEE Robotics and Automation Letters 1 (2) (2016) 938–945. doi:10.1109/LRA.2016.2531124.

[16] P. D. Labrecque, T. Laliberte, S. Foucault, M. E. Abdallah, C. Gosselin, uman: A low-impedance manipulator for human-robot cooperation based on underactuated redundancy, IEEE/ASME Transactions on Mechatronics PP (99) (2017) 1–1. doi:10.1109/TMECH.2017.2652322.

[17] P. Belanger, P. Dobrovolny, A. Helmy, X. Zhang, Estimation of angular velocity and acceleration from shaft-encoder measurements, The International Journal of Robotics Research 17 (11) (1998) 1225–1233.

[18] D. Gao, A. Lecours, T. Laliberte, S. Foucault, C. Gosselin, B. Mayer-St-Onge, , R. J. Menassa, P.-L. Belzile, Movement system configured for moving a payload, US Patent Application 13/664,947 (2012).

[19] A. Benaskeur, A. Desbiens, Application of adaptive backstepping to the stabilization of the inverted pendulum, in: IEEE Canadian Conference on Electrical and Computer Engineering, Vol. 1, 1998, pp. 113–116 vol.1.

[20] M. Mokhtari, N. Golea, S. Berrahal, The observer adaptive backstepping control for a simple pendulum, AIP Conference Proceedings 1019 (1) (2008) 85–90.